Organocatalytic Atroposelective Hydrochalcogenation of Alkynes to Access Axially Chiral Vinyl Chalcogenides

Yi-Xin Wang,[1,2] Jing-Run Wang,[1,2] Chen Cui,[1,2] Zhen Wang,[1,2] Yu Lu,[1,2,*] and Xiao-Hui Yang[1,2,3,*]

[1] Advanced Research Institute of Multidisciplinary Science, Beijing Institute of Technology, Zhuhai, Zhuhai 519088 (P. R. China)

[2]Advanced Research Institute of Multidisciplinary Science, and School of Chemistry and Chemical Engineering, Key Laboratory of Medical Molecule Science and Pharmaceutical Engineering, Ministry of Industry and Information Technology, Beijing Institute of Technology, Beijing 100081 (P. R. China)

[3]State Key Laboratory of Elemento-Organic Chemistry, Nankai University, Tianjin 300071 (P. R. China)

Abstract: The low racemization barrier inherent in axially chiral vinyl sulfides/selenides ($\Delta G^{\neq} \leqslant 26.8$ kcal/mol) poses a significant challenge for achieving atroposelective hydrochalcogenation of alkynes. In this study, we present an unprecedented atroposelective hydrochalcogenation of alkynes catalyzed by organocatalysts. This organocatalytic, atom-economic process proceeds under mild conditions and exhibits exceptional enantio-, regio-, and *E*-stereoselectivity. Insights from detailed Density Functional Theory (DFT) studies elucidate the origins of these high selectivities.

Introduction

Organochalcogenides demonstrate remarkable versatility and play a significant role in a wide range of applications, including pharmaceuticals, bioactive molecules, agrochemicals, and functional materials.[1-4] Moreover, in synthetic chemistry, organochalcogenides exhibit distinctive activities as chiral catalysts and ligands (Fig. 1a).[5-7] Despite the established high activities of chiral organochalcogenides, their synthesis presents a significant challenge due to the well-documented catalyst poisoning[8, 9]of sulfur and selenium. The enantioselective, atom-economic hydrochalcogenation of unsaturated hydrocarbons represents one of the most powerful and straightforward methods for synthesizing chiral organochalcogenides.[10-12] However, it is currently limited to the asymmetric hydrochalcogenation of alkenes, including Michael acceptors,[13, 14] 1,3-dienes,[15, 16] allenes,[17-19] cyclic alkenes,[20-22] and styrenes[23]. The enantioselective hydrochalcogenation of alkynes remains unexplored.

Axially chiral compounds have outstanding performance as chiral ligands and catalysts in asymmetric catalysis.[24-26] Although remarkable progress has been achieved in the synthesis of axially chiral (hetero)biaryl compounds,[27-32] catalytic atroposelective access to axially chiral alkenes remains challenging due to the low rotational barrier, weak atropostability, and difficulty in controlling the *E/Z*-stereoselectivity.[33-40] In 2017, Tan pioneered the catalytic atroposelective hydrofunctionalization of alkynes to access axially chiral alkenes.[41] Subsequently, Yan,[42] Houk & Tan, [43] Li,[44] Yang & Tan & Wang, [45] Gao & Yao,[46] and others,[47-50] further advanced atroposelective alkyne hydrofunctionalization, which provides an important solution to the aforementioned challenges (Fig. 1b). However, these atroposelective hydrofunctionalizations typically require bulky functionalizing reagents, such as hydrosulfonylation,[42] hydroarylation,[43] hydrophosphination,[44, 45] and hydrosilylation[46], which limit the resulting axially chiral alkenes to those with high racemization barriers ($\Delta G^{\neq} > 30$ kcal/mol). In contrast, atroposelective alkyne hydrochalcogenation presents additional challenges because the sterically less

hindered SR/SeR groups further lower the racemization barrier ($\Delta G^{\neq}$ = 25.6 kcal/mol and 26.8 kcal/mol, respectively). Inspired by asymmetric bifunctional organocatalyzed reactions,[51-53] we expected that the use of bifunctional organocatalysts, such as phosphoric acids and (thio)urea derivatives, could provide a potential solution to the challenge by synergistically activating alkynes and thiols/selenols through multiple hydrogen bond interactions. Based on this design consideration and our ongoing interest in the enantioselective hydrofunctionalization of unsaturated hydrocarbons,[54, 55] we present here an organocatalyzed regio- and atroposelective hydrochalcogenation of alkynes to generate axially chiral vinyl sulfides and selenides (Fig. 1c).[56] DFT calculations elucidate the reaction mechanism and the origin of the enantioselectivity and *E*-stereoselectivity.

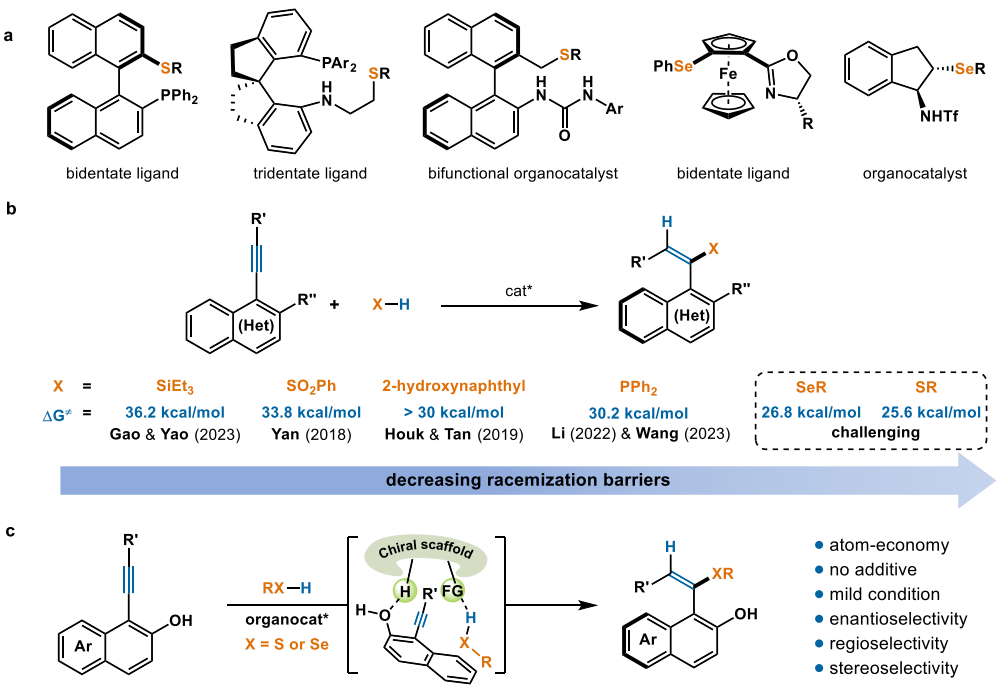

Fig. 1. Inspiration for atroposelective hydrochalcogenation of alkynes. a, selected chiral organochalcogenides as ligands and catalysts. **b**, typically atroposelective hydrofunctionalization of alkynes. **c**, **this work**: atroposelective hydrochalcogenation of alkynes.

Reaction development

We initiated our investigation using alkyne **1a** and thiol **2a** as model substrates. We explored a range of bifunctional organocatalysts featuring diverse chiral frameworks and functional groups, and the representative results are shown in Table 1. Chiral phosphoric acid **C1** smoothly promoted hydrothiolation to afford axially chiral sulfides **3aa** in 78% yield with 45:55 *er*. Encouraged by this result, we set out to investigate a series of axially chiral phosphoric acids (**C2–C5**), among which the sterically bulky phosphoric acid **C5** significantly increased the enantioselectivity to 10:90 *er* with high yield (75%). Subsequently, various chiral thiourea and urea derivatives (**C6–C10**) were evaluated. In particular, the quinine-derived urea **C10** efficiently catalyzed the hydrothiolation and provided the desired product **3aa** in excellent yield (98%) with good enantioselectivity (85:15 *er*) at room temperature. To our delight, when the temperature was lowered to 0 °C, the enantioselectivity was increased to 97:3 *er* with excellent yield (98%). Overall, this represents the first example of atroposelective hydrothiolation of alkynes.

Table 1. Reaction optimization.

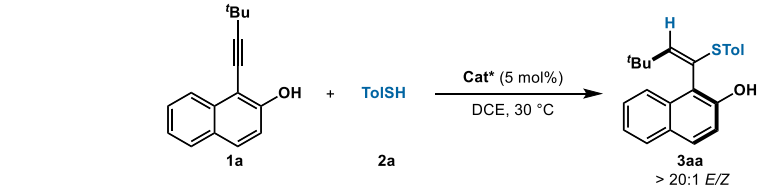

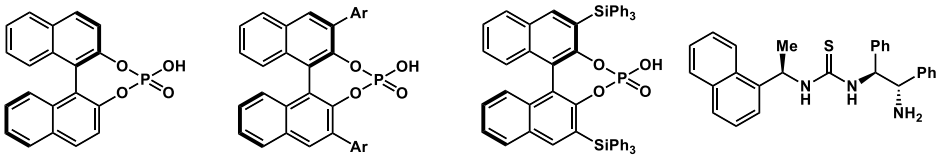

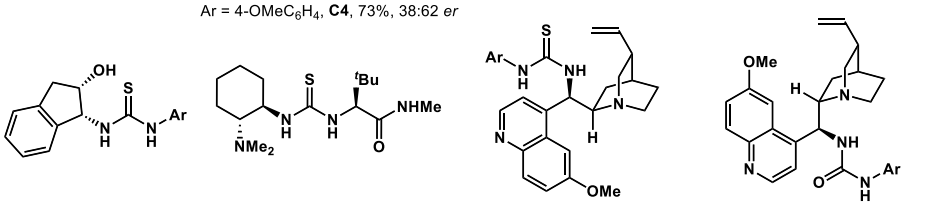

Reaction condition: **1a** (0.1 mmol), **2a** (0.15 mmol), **Cat*** (5 mol%), 1,2-dichloroethane (DCE, 0.4 mL), 30 °C, 5 h. Isolated yield. Regioselectivity and stereoselectivity were determined by ^{1}H NMR analysis of the unpurified reaction mixture. Enantiomeric ratio (*er*) was determined by chiral HPLC. Tol = 4-MeC_6H_4, Ar = 3,5-$(CF_3)_2C_6H_3$.

Scope for hydrothiolation

After establishing the optimal reaction conditions, we explored the generality of the hydrothiolation reaction. Under the standard conditions, we first examined the addition of various thiols **2** to alkyne **1a** (Table 2). Thiols with both electron-donating and electron-withdrawing groups on the phenyl rings reacted smoothly, yielding the desired products with high yields and enantioselectivity (**3ab**–**3ak**, 70−97% yield, 90:10−98:2 *er*). Additionally, this methodology is compatible with heteroaromatic rings, including furan (**3al**, 98% yield, 98:2 *er*), thiophene (**3am**, 52% yield, 96:4 *er*), and benzimidazole (**3an**, 98% yield, 99:1 *er*). The absolute configuration of the product **3an** was determined to be (*S*) by X-ray crystallographic analysis. Initially, attempts to extend the reaction to aliphatic thiols were unsuccessful, as the enantioselectivity of the product decreased significantly over time. However, the use of phosphonic the acid catalyst **C5** in place of the urea catalyst **C10** enabled successful hydrothiolation with aliphatic thiol **2o**, giving the product **3ao** in 67% yield with 89:11 *er*. In all cases, only a single constitutional isomer was obtained.

Subsequently, we examined the hydrothiolation of various alkynes with thiol **2a**. Substituents such as methoxy, halogen, and trifluoromethyl on the naphthalene ring were found to be compatible, yielding the desired axially chiral vinyl thioethers in high yields and with excellent enantioselectivities (**3ba**–**3ga**, 70−99% yield, 94:6−96:4 *er*). Notably, the hydrothiolation of 1,7-bisalkynyl 2-naphthalenol selectively afforded the expected products **3ha** in 60% yield and 94:6 *er*, with no observed side product formation from the hydrothiolation of the 7-alkynyl groups. This result indicates the essential role of the *ortho*-hydroxyl group in the activation of the alkyne. Furthermore, the replacement of the tertiary butyl group with the less sterically hindered cyclohexyl and *n*-butyl groups met with no difficulty, and the products were all isolated in high yields and enantioselectivities (**3ia** and **3ja**).

Table 2. Scope for Atroposelective Hydrothiolation.

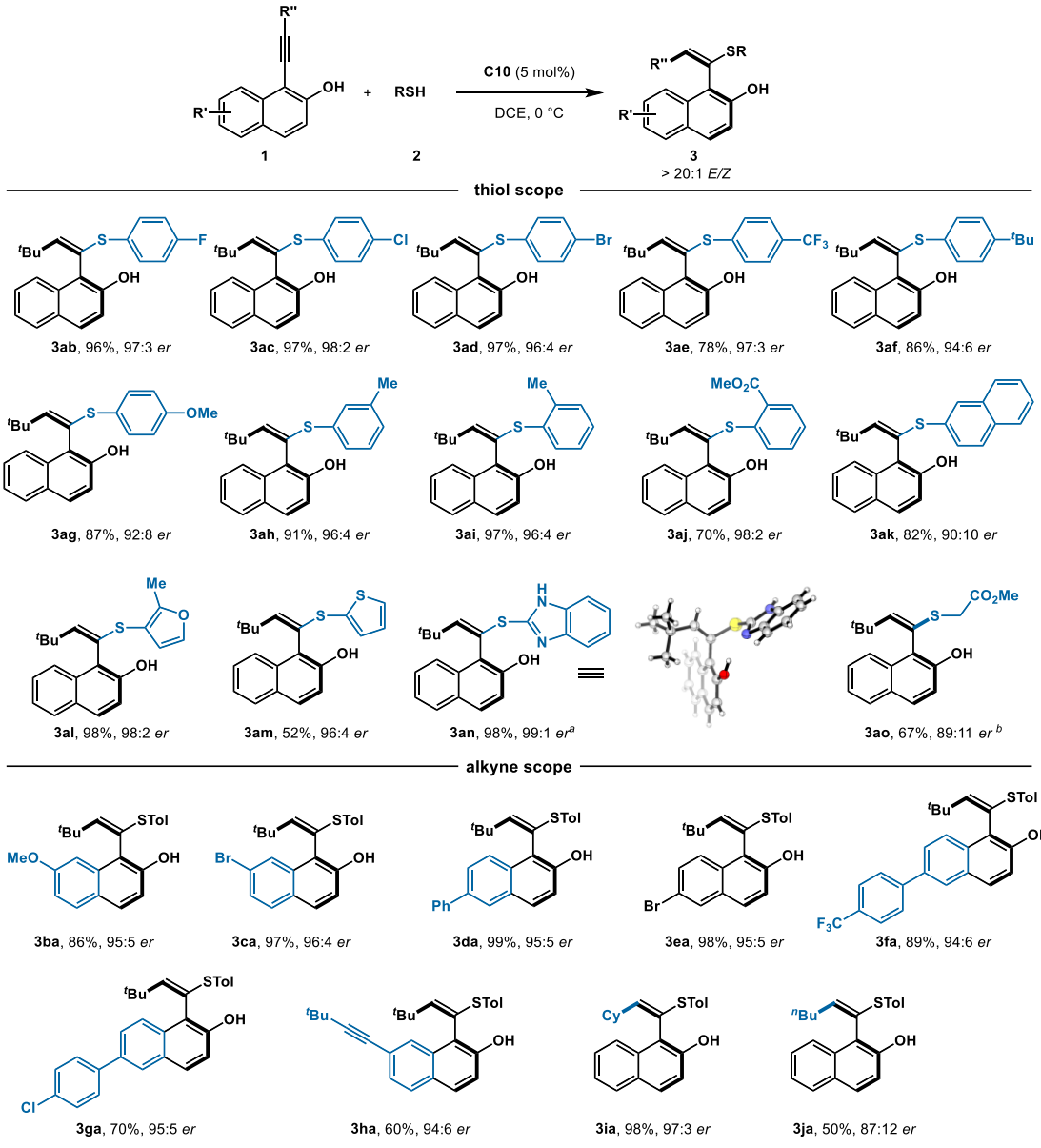

Isolated yield.Regioselectivity and stereoselectivity were determined by ^{1}H NMR analysis of the unpurified reaction mixture. *er* was determined by chiral HPLC. [a] 30 °C. [b] using **C5**

Scope for hydroselenation

We also investigated the hydroselenation, and the quinidine-derived thiourea **C9** was found to give the best results (Table 3). Hydroselenation with selenols bearing electron-donating groups showed high reactivity and excellent enantioselectivity (**5ab**–**5ad**, 82–98% yield, 95:5–99:1 *er*). However, selenols containing electron-withdrawing groups on the phenyl ring showed poor reactivity under the optimized conditions. Encouragingly, switching the catalyst from thiourea **C9** to phosphoric acid **C5** successfully facilitated the transformation and provided the desired axially chiral vinyl selenides with high reactivity and enantioselectivity (**5ae**–**5ag**, 78–87% yield, 90:10–98:2 *er*). In addition, this protocol tolerated *ortho*- and *meta*-substituted selenols (**5ah** and **5ai**). Hydroselenation with bulky selenol **4j** also proceeded well and delivered axially chiral selenides with good results (**5aj**, 64% yield, 93:7 *er*). Aliphatic selenols did not react under these conditions. It is noteworthy to point out that all products from this

transformation showed complete *E*-stereoselectivity (>20:1 *E/Z*).

Next, we explored the hydroselenation of various alkynes with selenol **4a**. Under optimized conditions, various functional groups on the naphthalene rings are well tolerated and the desired chiral selenides were obtained in moderate to high yields with excellent enantioselectivity (**5aa**–**5ga**, 51–98% yield, 87:13–99:1 *er*). The hydroselenation of alkynes can also be achieved selectively at the *ortho*-hydroxyl position, even in the presence of multiple triple bonds (**5ha**, 77% yield and 95:5 *er*). When the *tert*-butyl group at the alkyne was replaced with the smaller cyclohexyl and *n*-butyl groups, the transformation also proceeded smoothly, generating axially chiral selenides (**5ia** and **5ja**) with good reactivity (61% and 78% yield, respectively) and enantioselectivity (94:6 *er* and 99:1 *er*, respectively).

Table 3. Scope for Atroposelective Hydroselenation.

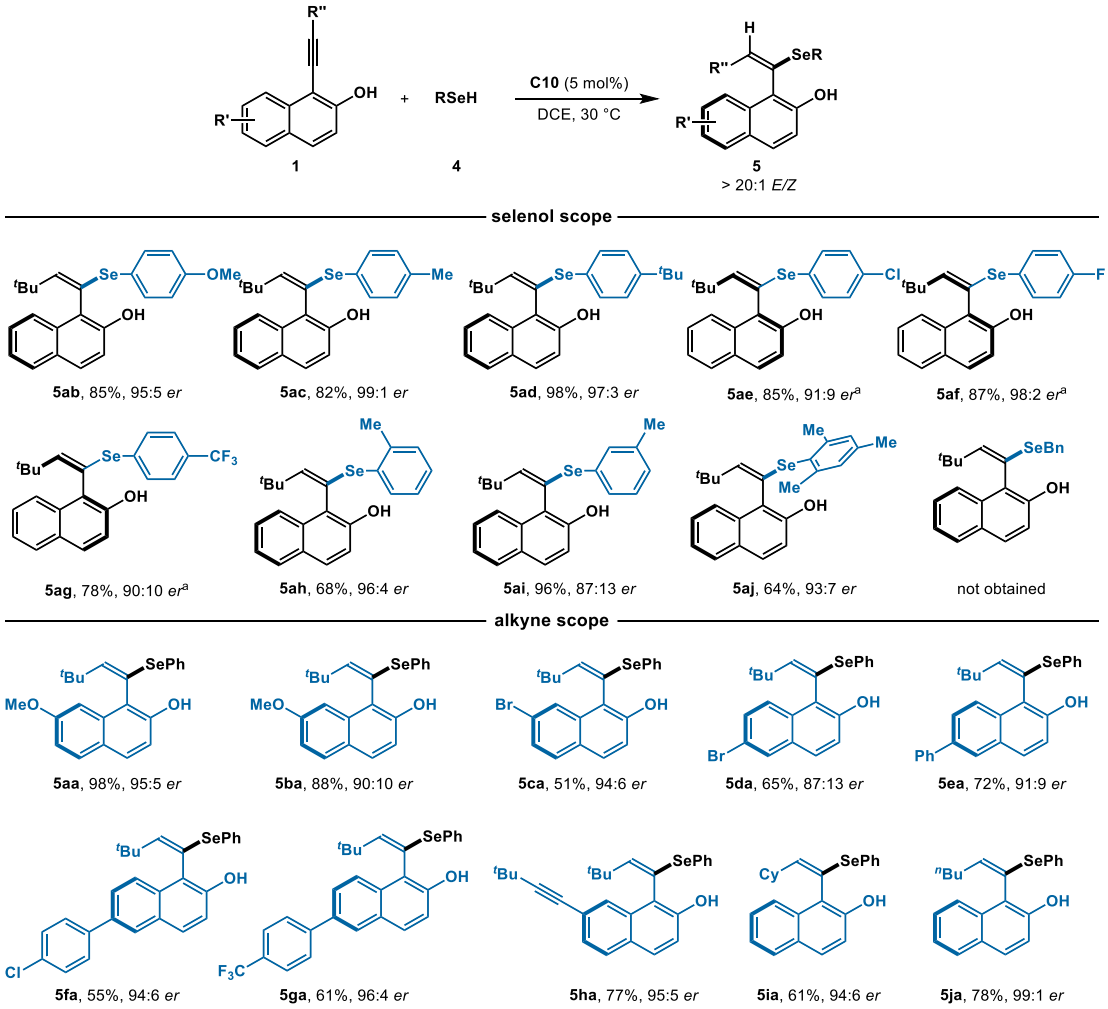

Isolated yield. Regioselectivity and stereoselectivity were determined by ^{1}H NMR analysis of the unpurified reaction mixture. *er* was determined by chiral HPLC. [a] using **C5**, 4 h.

Transformations

To demonstrate the potential utility of our protocol, we synthesized **3aa** and **5aa** on a gram scale with no erosion of the yield or enantioselectivity using a catalyst loading as low as 1 mol% (Fig. 2a). The chiral sulfide **3aa** and selenide **5aa** were readily oxidized to the corresponding sulfone **6** and selenone **7** (Fig. 2b). Additionally, the potential S/P **8** and Se/P **9** ligand were synthesized in high yield by reacting the axially chiral sulfide **3aa** or selenide **5aa** with chlorodiphenylphosphine (Fig. 2c). The cross-coupling

reaction of vinyl thioethers/selenides with various reagents facilitates the conversion of C–S/Se bonds into a diverse range of C–X bonds.[57, 58] For example, product **10** was successfully synthesized via the Kumada coupling of **3aa** or **5aa** with a Grignard reagent (Fig. 2d).

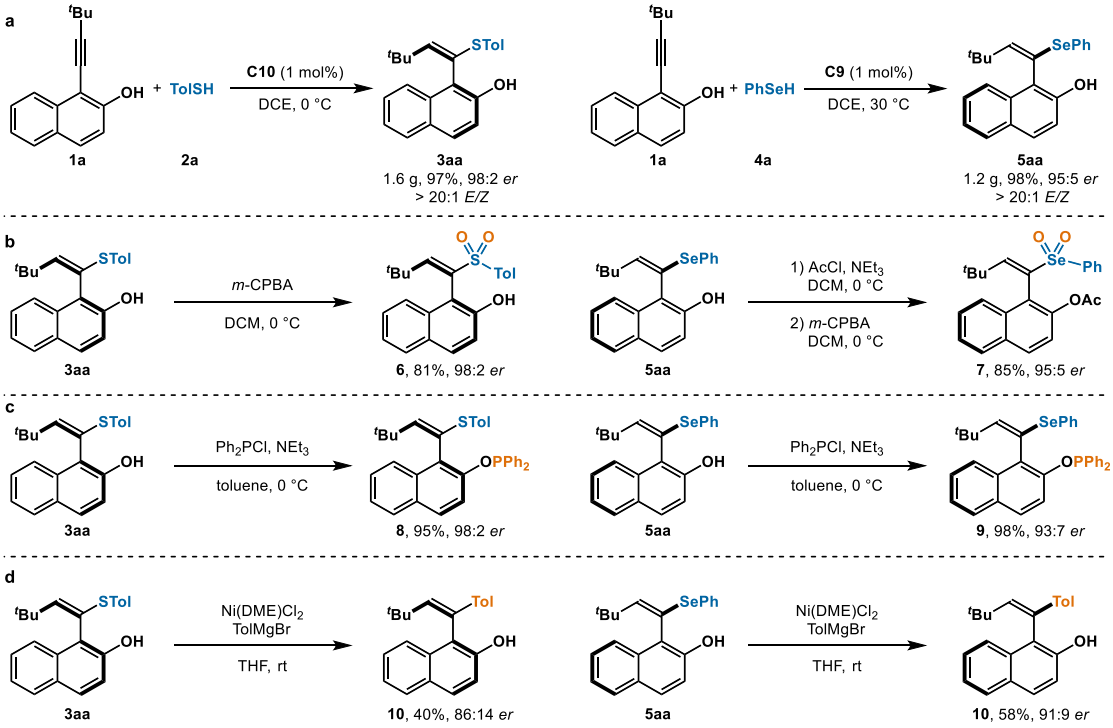

Fig. 2. Gram-scale reaction and transformations. a, gram-scale reactions. **b,** oxidation of axially chiral vinyl thiolethers and selenides. **c,** synthesis of potential S/P and Se/P ligand. **d,** cross-coupling of axially chiral vinyl thiolethers and selenides.

Mechanism investigation

To explore the reaction mechanism and gain insight into the origin of the enantioselectivity and *E*-stereoselectivity, DFT calculations were performed on the **C10**-catalyzed hydrothiolation between **1a** and **2a**. Based on our computational results and previous reports [42, 43, 51-53, 59, 60], we propose that the chiral urea serves as a bifunctional organocatalyst to synergistically activate alkynes and thiols. As illustrated in Fig. 3a, deprotonation of alkyne **1a** by **C10** leads to the formation of an ammonium intermediate **Int1**, where the naphthalenolate anion is stabilized by multiple hydrogen bond interactions.[51-53] Proton transfer then occurs via **TS1-R** (18.5 kcal/mol) to yield the electrophilic (*R*)-vinylidene *ortho*-quinone methide (VQM)[59, 60] **Int2-R**. Subsequently, thiol **2a** associates with **Int2-R** to form **Int3** via an N···H–S hydrogen bond. This is followed by deprotonation of the thiol via **TS2** (18.0 kcal/mol) to give **Int4**. Nucleophilic attack of the sulfur anion on (*R*)-VQM from the opposite side of the bulky *tert*-butyl group of the allene (*E* face) produces the intermediate **Int5** via **TS3** (22.5 kcal/mol), which is the rate-determining step. Subsequent protonation yields the desired product **3aa** and regenerates the free catalyst **C10**.

To elucidate the origin of the enantioselectivity, we also calculated the formation of (*S*)-VQM **Int2-S** (red pathway), which is energetically disfavored by 11.1 kcal/mol compared to the transition state **TS1-R**. We further investigated the origin of enantioselectivity by a visual analysis of non-covalent interactions (NCIs)[61, 62] (Fig. 3b). A significant difference in **1a**···**C10** nonbonding interactions is observed between **TS1-R** and **TS1-S**. The *tert*-butyl group and the naphthalene ring of **1a** can interact

with **C10** through a variety of C–H···π/π···π interactions (the green region) in **TS1-R**. Conversely, a strong steric repulsion (the red region) is observed between **1a** and **C10** in **TS1-S**. Additionally, we calculated the catalyst distortion energies (energy difference between the catalyst fragment in the transition structure and **C10**, $\Delta E^{\ddagger}_{dist}$) of **TS1-R** and **TS1-S**. The distortion energy of **TS1-S** (10.5 kcal/mol) is higher than that of **TS1-R** (4.7 kcal/mol). Overall, these results support that the formation of (*R*)-VQM **Int2-R** is more favorable than (*R*)-VQM **Int2-S**.

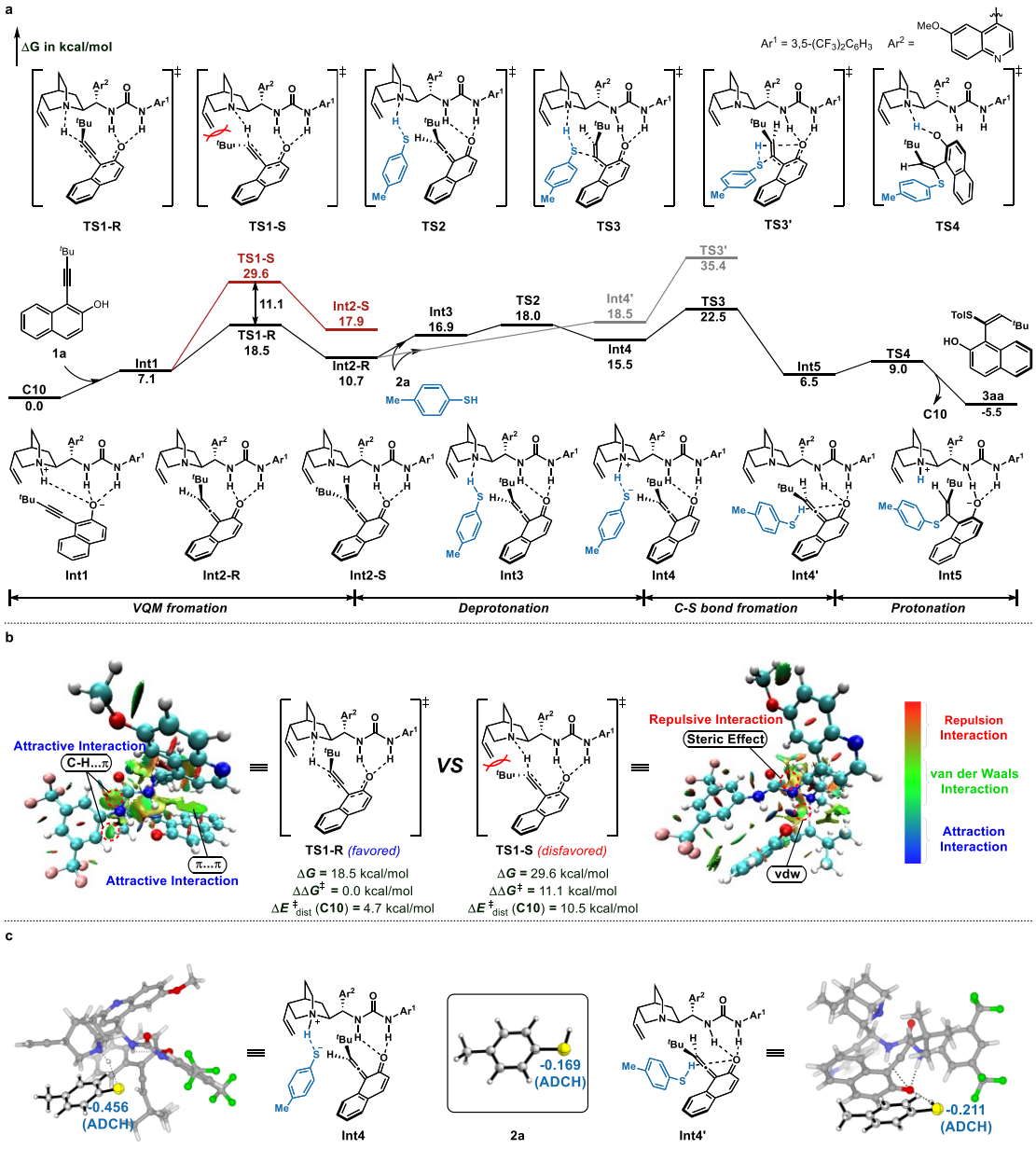

Fig. 3. DFT calculations. a, energy profile. **b**, NCIs analyses and the distortion energies of catalyst. **c**, ADCH atomic charge of S.

Finally, to shed light on the origin of the *E*-stereoselectivity, we also calculated the free energy profile for the formation of *Z*-**3aa** (gray pathway, Fig. 3a). Thiol **2a** associates with the intermediate **Int2-R** to form **Int4'** via an O···H–S hydrogen bond. The nucleophilic attack of thiol on **Int2-R** occurs from the same side of the bulky *tert*-butyl group of the allene (*Z* face) to give *Z*-**3aa** via **TS3'** (35.4 kcal/mol). **TS3'** is energetically less favorable than **TS3** by 12.9 kcal/mol. This discrepancy in free energy can be

attributed to two factors: 1) steric repulsion between the *tert*-butyl group and the PhS group in **TS3'**, and 2) weaker nucleophilicity of the S center in **TS3'**. Atomic dipole moment corrected Hirshfeld (ADCH) charge population analysis[63] indicates that the S atom in **Int4** (-0.456) is more negatively charged compared to the S atom in both thiol **2a** (-0.169) and **Int4'** (-0.211) (Fig. 3c). The increased nucleophilicity of S atom in **Int4** lowers the energy barrier for the formation of *E*-**3aa** compared to that for *Z*-**3aa**.

Conclusion

The atroposelective hydrochalcogenation of alkynes is challenging due to the low rotational barrier and weak atropostability of axially chiral vinyl sulfides/selenides. By using organocatalysis, we successfully achieved the first atroposelective hydrochalcogenation of alkynes. This atom-economic process is conducted under mild conditions and demonstrates excellent enantio-, regio-, and *E*-stereoselectivity. DFT studies shed light on the reaction mechanism and the origin of these high selectivities.

Methods

General procedure for hydrochalcogenation of alkynes

In a N_2-filled glovebox, alkyne (0.1 mmol) and thiol/selenol (0.15 mmol) were added to a solution of catalyst (0.005 mmol) in DCE (0.40 mL) in a 1-dram vial. The resulting mixture was stirred at 0 ^oC or 30 ^oC until no starting material was observed by TLC or GC. The reaction mixture was then concentrated and purified by flash silica gel chromatography to give the pure product.

Data availability

All other data are available from the corresponding author upon request. For experimental details and procedures, spectra for all unknown compounds, see supplementary files.

References

1. Engman, L., Stern, D., Frisell, H., Vessman, K., Berglund, M., Ek, B. & Andersson, C. M. Synthesis, antioxidant properties, biological activity and molecular modelling of a series of chalcogen analogues of the 5-lipoxygenase inhibitor DuP 654. *Bioorg. Med. Chem.* **3**, 1255–1262 (1995).
2. Rosati, O. Organochalcogen Compounds: Synthesis and Prospective as Therapeutic Agents. *Curr. Med. Chem*. **30**, 2355–2356 (2023).
3. Xu, H., Cao, W. & Zhang, X. Selenium-Containing Polymers: Promising Biomaterials for Controlled Release and Enzyme Mimics. *Acc. Chem. Res.* **46**, 1647–1658 (2013).
4. Devendar, P. & Yang, G. F. Sulfur-containing agrochemicals. *Top. Curr. Chem.* **375**, 1–44 (2017).
5. Shao, L., Li, Y., Lu, J. & Jiang, X. Recent progress in selenium-catalyzed organic reactions. *Org. Chem. Front.* **6**, 2999–3041 (2019).
6. Liao, L. & Zhao, X. Indane-Based Chiral Aryl Chalcogenide Catalysts: Development and Applications in Asymmetric Electrophilic Reactions. *Acc. Chem. Res.* **55**, 2439−2453 (2022).
7. Nishiyori, R., Mori, T., Okuno, K. & Shirakawa, S. Chiral sulfide and selenide catalysts for asymmetric halocyclizations and related reactions. *Org. Biomol. Chem.* **21**, 3263−3275 (2023).

8. Yamamoto, Y. & Ogawa, A. Transition-Metal-Catalyzed Addition of Organosulfur Compounds to Alkynes and Alkenes: Catalysis and Catalyst Poisons. *Chem. Eur. J.* **29**, e202302432 (2023).

9. Dunleavy, J. Sulfur as a catalyst poison. *Platinum Met. Rev*. **50**, 110 (2006).

10. Beletskaya, I. P. & Ananikov, V. P. Transition-metal-catalyzed C–S, C–Se, and C–Te bond formations via cross-coupling and atom-economic addition reactions. *Chem. Rev*. **122**, 16110–16293 (2022).

11. Castarlenas, R., Di Giuseppe, A., Pérez-Torrente, J. J. & Oro, L. A. The Emergence of Transition-Metal-Mediated Hydrothiolation of Unsaturated Carbon–Carbon Bonds: A Mechanistic Outlook. *Angew. Chem. Int. Ed.* **52**, 211–222 (2013).

12. Ogawa, A. Transition-Metal-Catalyzed S–H and Se–H Bonds Addition to Unsaturated Molecules. *Top Organomet. Chem.* **43**, 325–360 (2013).

13. Li, E., Chen, J. & Huang, Y. Enantioselective Seleno−Michael Addition Reactions Catalyzed by a Chiral Bifunctional N−Heterocyclic Carbene with Noncovalent Activation. *Angew. Chem. Int. Ed.* **61**, e202202040 (2022).

13. Tian, H., Zhang, H.-M. & Yin, L. Copper(I)-Catalyzed Conjugate Addition/Enantioselective Protonation with Selenols and α-Substituted α, β-Unsaturated Thioamides. *Angew. Chem. Int. Ed.* **62**, e202301422 (2023).

15. Yang, X.- H., Davison, R. T. & Dong, V. M. Catalytic Hydrothiolation: Regio and Enantioselective Coupling of Thiols and Dienes. *J. Am. Chem. Soc.* **140**, 10443−10446 (2018).

16. Yang, X.-H., Davison, R. T., Nie, S.-Z., Cruz, F. A., McGinnis, T. M. & Dong, V. M. Catalytic Hydrothiolation: Counterion-Controlled Regioselectivity. *J. Am. Chem. Soc.* **141**, 3006−3013(2019).

17. Han, X., Wang, M., Liang, Y., Zhao, Y. & Shi. Z. Regio- and enantioselective nucleophilic addition to *gem*-difluoroallenes. *Nat. Syn*. **1**, 227−234 (2022).

18. Pritzius, A. B. & Breit, B. Asymmetric Rhodium-Catalyzed Addition of Thiols to Allenes: Synthesis of Branched Allylic Thioethers and Sulfones. *Angew. Chem. Int. Ed.* **54**, 3121−3125 (2015).

19. Pritzius, A. B. & Breit, B. *Z*-Selective Hydrothiolation of Racemic 1,3-Disubstituted Allenes: An Atom-Economic Rhodium-Catalyzed Dynamic Kinetic Resolution. *Angew. Chem. Int. Ed.* **54**, 15818−15822 (2015).

20. Nie, S., Lu, A., Kuker, E. L. & Dong, V. M. Enantioselective Hydrothiolation: Diverging Cyclopropenes through Ligand Control. *J. Am. Chem. Soc*. **143**, 6176−6184 (2021).

21. Li, S., Lu, Z., Meng, L. & J. Wang. Iridium-Catalyzed Asymmetric Addition of Thiophenols to Oxabenzonorbornadienes. *Org. Lett.* **18**, 5276−5279 (2016).

22. Li, S., Yang, Q., Bian, Z. & Wang, J. Rhodium−Catalyzed Enantioselective Hydroselenation of Heterobicyclic Alkenes. *Org. Lett.* **22**, 2781−2785 (2020).

23. Slocumb, H. S., Nie, S., Dong, V. M. & Yang, X.−H. Enantioselective Selenol-ene Using Rh-Hydride Catalysis. *J. Am. Chem. Soc.* **144**, 18246−18250 (2022).

24. Kumarasamy, E., Raghunathan, R., Sibi, M. P. & Sivaguru, J. Nonbiaryl and Heterobiaryl Atropisomers: Molecular Templates with Promise for Atropselective Chemical Transformations. *Chem. Rev.* **115**, 11239−11300 (2015).

25. Akiyama, T. & Mori, K. Stronger Brønsted acids: recent progress. *Chem. Rev.* **115**, 9277–9306 (2015).

26. Yue, Q., Liu, B., Liao, G. & Shi, B.-F. Binaphthyl Scaffold: A Class of Versatile Structure in Asymmetric C−H Functionalization. *ACS Catal.* **12**, 9359−9396 (2022).

27. Carmona, J. A., Rodríguez-Franco, C., Fernández, R., Hornillos, V. & Lassaletta, J. M. Atroposelective transformation of axially chiral (hetero)biaryls. From desymmetrization to modern resolution strategies. *Chem. Soc. Rev.* **50**, 2968–2983 (2021).

28. Kitagawa, O. Chiral Pd-Catalyzed Enantioselective Syntheses of Various N−C Axially Chiral Compounds and Their Synthetic Applications. *Acc. Chem. Res.* **2021**, *54*, 719−730.

29. Liu, C.-X., Zhang, W.-W., Yin, S.-Y., Gu, Q. & You, S.-L. Synthesis of Atropisomers by Transition-Metal-Catalyzed Asymmetric C-H Functionalization Reactions. *J. Am. Chem. Soc*. **143**, 14025–14040 (2021).

30. Cheng, J. K., Xiang, S.-H. & Tan, B. Organocatalytic Enantioselective Synthesis of Axially Chiral Molecules: Development of Strategies and Skeletons. *Acc. Chem. Res.* **55**, 2920−2937 (2022).

31. Zhang, H.-H. & Shi, F. Organocatalytic Atroposelective Synthesis of Indole Derivatives Bearing Axial Chirality: Strategies and Applications. *Acc. Chem. Res*. **55**, 2562–2580 (2022).

32. Xiang, S.-H., Ding, W.-Y., Wang, Y.-B. & Tan, B. Catalytic atroposelective synthesis, *Nat. Catal.* **7**, 483–498 (2024).

33. Feng, J.; Gu, Z. Atropisomerism in Styrene: Synthesis, Stability, and Applications. *SynOpen* **5**, 68–85(2021).

34. Qian, P.-F., Zhou, T. & Shi, B.-F. Transition-metal-catalyzed atroposelective synthesis of axially chiral styrenes. *Chem. Commun.* **59**, 12669–12684 (2023).

35. Li, Z.-H., Li, Q.-Z., Bai, H.-Y. & Zhang, S.-Y. Synthetic strategies and mechanistic studies of axially chiral styrenes. *Chem Catal.* **3**, 100594 (2023).

36. Wang, J., Qi, X., Min, X.-L.,Yi, W.; Liu, P. & He, Y. Tandem iridium catalysis as a general strategy for atroposelective construction of axially chiral styrenes. *J. Am. Chem. Soc*. **143**, 10686–10694 (2021).

37. Yokose, D., Nagashima, Y.,Kinoshita, S., Nogami, J. &Tanaka, K. Enantioselective Synthesis of Axially Chiral Styrene-Carboxylic Esters by Rhodium-Catalyzed Chelation-Controlled [2+2+2] Cycloaddition. *Angew. Chem. Int. Ed.* **61**, e202202542 (2022).

38. Fu, L., Chen, X., Fan, W., Chen, P. & Liu, G. Copper-Catalyzed Asymmetric Functionalization of Vinyl Radicals for the Access to Vinylarene Atropisomers. *J. Am. Chem. Soc*. **145**, 13476–13483 (2023).

39. Wu, F., Zhang, Y., Zhu, R. & Huang, Y. Discovery and synthesis of atropisomerically chiral acyl-substituted stable vinyl sulfoxonium ylides. *Nat. Chem.* **16**, 132–139 (2024).

40. Ma, X., Tan, M., Li, L., Zhong, Z., Li, P., Liang, J. & Song, Q. Ni-catalysed assembly of axially chiral alkenes from alkynyl tetracoordinate borons via 1,3-metallate shift. *Nat. Chem.* **16**, 42–53 (2024).

41. Zheng, S.-C., Wu, S., Zhou, Q., Chung, L. W., Ye, L. & Tan, B. Organocatalytic atroposelective synthesis of axially chiral styrenes. *Nat. Commun.* **8**, 15238 (2017).

42. Jia, S., Chen, Z., Zhang, N., Tan, Y., Liu, Y., Deng, J. & Yan, H. Organocatalytic enantioselective construction of axially chiral sulfone-containing styrenes. *J. Am. Chem. Soc.* **140**, 7056–7060 (2018).

43. Wang, Y.-B., Yu, P., Zhou, Z.-P., Zhang, J., Wang, J., Luo, S.-H., Gu, Q.-S., Houk, K. N. & Tan, B. Rational design, enantioselective synthesis and catalytic applications of axially chiral EBINOLs. *Nat. Catal.* **2**, 504–513 (2019).

44. Ji, D., Jing, J., Wang, Y., Qi, Z., Wang, F., Zhang, X., Wang, Y. & Li, X. Palladium-catalyzed asymmetric hydrophosphination of internal alkynes: Atroposelective access to phosphinefunctionalized olefins. *Chem* **8**, 3346–3362 (2022).

45. Cai, B., Cui, Y., Zhou, J., Wang, Y.-B., Yang, L., Tan, B. & Wang, J. Asymmetric Hydrophosphinylation of Alkynes: Facile Access to Axially Chiral Styrene-Phosphines. *Angew. Chem. Int. Ed.* **62**, e202215820 (2023).

46. Wu, Q., Zhang, Q., Yin, S., Lin, A., Gao, S. & Yao, H. Atroposelective Synthesis of Axially Chiral Styrenes by Platinum-Catalyzed Stereoselective Hydrosilylation of Internal Alkynes. *Angew. Chem. Int. Ed.* **62**, e202305518 (2023).

47. Li, Q.-Z., Lian, P.-F., Tan, F.-X., Zhu, G.-D., Chen, C., Hao, Y., Jiang, W., Wang, X.-H., Zhou, J. & Zhang, S.-Y. Organocatalytic Enantioselective Construction of Heterocycle-Substituted Styrenes with Chiral Atropisomerism. *Org. Lett*. **22**, 2448−2453 (2020).

48. Yan, J.-L., Maiti, R., Ren, S.-C., Tian, W., Li, T., Xu, J., Mondal, B., Jin, Z. & Chi, Y. R. Carbene-catalyzed atroposelective synthesis of axially chiral styrenes. *Nat. Commun.* **2022**, *13*, 84.

49. Sheng, F.-T., Wang, S.-C., Zhou, J., Chen, C., Wang, Y. & Zhu, S. Control of Axial Chirality through NiH-Catalyzed Atroposelective Hydrofunctionalization of Alkynes. *ACS Catal*. **13**, 3841−3846 (2023).

50. Zhan, L.-W.; Lu, C.-J.; Feng, J.; Liu, R.-R. Atroposelective Synthesis of C-N Vinylindole Atropisomers by Palladium-Catalyzed Asymmetric Hydroarylation of 1-Alkynylindoles. *Angew. Chem. Int. Ed*. **62**, e202312930 (2023).

51. Fang, X. & Wang, C.-J. Recent advances in asymmetric organocatalysis mediated by bifunctional amine–thioureas bearing multiple hydrogen-bonding donors. *Chem. Commun.* **51**, 1185–1197 (2015).

52. Mukhopadhyay, S., Gharui, C. & Pan, S. C. Applications of Bifunctional Organocatalysts on ortho-Quinone Methides. *Asian J. Org. Chem.* **8**, 1970–1984 (2019).

53. Vera, S., García-Urricelqui, A., Mielgo, A. & Oiarbide, M. Progress in (Thio)urea- and Squaramide-Based Brønsted Base Catalysts with Multiple H-Bond Donors. *Eur. J. Org. Chem*. **26**, e202201254 (2023).

54. Jiu, A. Y., Slocumb, H. S., Yeung, C. S., Yang, X.-H. & Dong, V. M. Enantioselective Addition of Pyrazoles to Dienes. *Angew. Chem. Int. Ed*. **60**, 19660–19664 (2021).

55. Li, Q., Wang, Z., Dong, V. M. & Yang, X.-H. Enantioselective Hydroalkoxylation of 1,3-Dienes via Ni-Catalysis. *J. Am. Chem. Soc.* **145**, 3909–3914 (2023).

56. Zheng, D.-S., Xie, P.-P., Zhao, F., Zheng, C., Gu, Q., & You, S.-L. Rh(III)-Catalyzed Atroposelective C−H Selenylation of 1-Aryl Isoquinolines. *ACS Catal.* **14**, 6009−6015 (2024).

57. Stein, A. L., Bilheria, F. N. & Zeni, G. Application of organoselenides in the Suzuki, Negishi,

Sonogashira and Kumada cross-coupling reactions. *Chem. Commun*. **51**, 15522–15525 (2015).

58. Lou, J., Wang, Q., Wu, P., Wang, H., Zhou, Y.-G. & Yu, Z. Transition-Metal Mediated Carbon−Sulfur Bond Activation and Transformations: an Update. *Chem. Soc. Rev.* **49**, 4307−4359 (2020).

59. Rodriguez, J. & Bonne, D. Enantioselective organocatalytic activation of vinylidene−quinone methides (VQMs). *Chem. Commun.* **55**, 11168−11170 (2019).

60. Qin, W.; Liu, Y.; Yan, H. Enantioselective Synthesis of Atropisomers via Vinylidene *ortho*-Quinone Methides (VQMs). *Acc. Chem. Res.* **55**, 2780−2795 (2022).

61. Johnson, E. R. et al. Revealing Noncovalent Interactions. *J. Am. Chem. Soc.* **132**, 6498−6506 (2010).

62. Lu, T. & Chen, F. Multiwfn: A Multifunctional Wavefunction Analyzer. *J. Comput. Chem.* **33**, 580−592 (2012).

63. Lu, T. & Chen, F. Atomic Dipole Moment Corrected Hirshfeld Population Method. *J. Theor. Comput. Chem.* **11**, 163−183 (2012).

Acknowledgements

We thank the National Natural Science Foundation of China (Nos. 22201018 & 22371016), Beijing Natural Science Foundation (No.2222024), and the National Key Research and Development Program of China (No.2021YFA1401200) for funding. We thank the Analysis & Testing Center of Beijing Institute of Technology.

Author contributions

Y.-X.W. performed the most of experiments. C.C, and Z.W. synthesized some substrates. J.-R.W. and Y.L. performed DFT calculations. X.-H.Y. directed the project and wrote the manuscript with the feedback from all authors.

Competing interests

The authors declare no competing interests.